

Luminescence of Trivalent Lanthanide Ions Excited by Single-Bubble and Multibubble Cavitations

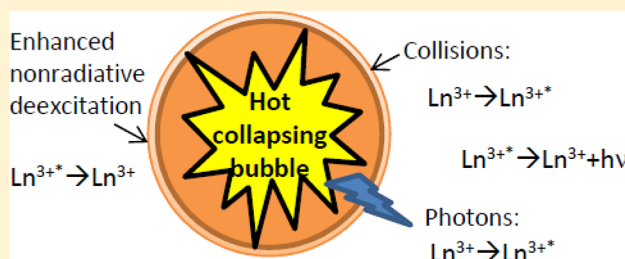
Rachel Pflieger,^{*,†,||} Julia Schneider,^{†,‡,§,||} Bertrand Siboulet,[†] Helmuth Möhwald,[‡] and Sergey I. Nikitenko[†]

[†]Institut de Chimie Séparative de Marcoule (ICSM), UMR 5257, BP 17171 - 30207 Bagnols-sur-Cèze Cedex, France

[‡]Max Planck Institute of Colloids and Interfaces, Am Mühlenberg 1, 14476 Potsdam, Germany

S Supporting Information

ABSTRACT: This article focuses on the possibility of exciting some lanthanides (Ce^{3+} , Tb^{3+} , Gd^{3+} , and Eu^{3+}) by ultrasound in aqueous solutions. Depending on the lanthanide ions and on the acoustic cavitation conditions (single-bubble or multibubble systems), the excitation mechanism is shown to be photo-excitation (e.g., for Ce^{3+}) or collision-induced excitation (e.g., for Tb^{3+}). The sonoluminescence of Tb^{3+} is studied in detail at various ultrasonic frequencies, allowing quantification of the amount of quenching. The latter is much stronger in sonoluminescence than in photoluminescence due to the particular properties of acoustic cavitation. Complexation with citrate ions enhances manifold sonoluminescence of lanthanides due to reduction of intra- and inner-molecular quenching.



1. INTRODUCTION

Because of their particular fluorescence/phosphorescence properties, lanthanides are widely used as optical emissive probes for medical diagnostics, in optics, as well as in catalysis.¹ Power ultrasound (US) is applied in similar fields, like medical diagnostics and treatments,² synthesis,³ and catalysis.⁴ Therefore, it appears interesting to look at the possibility of coupling ultrasound and lanthanides and take advantage of the properties of both. Actually, coupling of ultrasound and lanthanides (Ln^{3+}) is also of particular interest because these ions can be excited by two mechanisms, both of which can be provided by ultrasound. The first excitation pathway, sonophotoluminescence (SPL), is by photons emitted by cavitation bubbles at collapse.⁵ The second excitation pathway is by collisions with the “hot” particles generated during bubble collapse,⁶ similarly to what happens under α -, β -, or X-ray irradiation.⁷ In radiation chemistry, the impact generates excited water molecules that then transfer their energy to the lanthanide ions; alternatively, excited ions can also be produced by direct action of the radiation.⁸ In sonochemistry, direct excitation by collision and transfer of kinetic and excitation energy from the “hot” particles occurs in the bubble or at its interface.

Up to now, only one research group studied lanthanide sonoluminescence, using low-frequency 20 kHz ultrasound and low-resolution spectrometer.^{6,7,9} Because the ultrasonic frequency is known to control chemical and sonoluminescence activity,¹⁰ it would be of particular interest to compare lanthanide SL at various ultrasonic frequencies. Moreover, a comparison with a single-bubble (SB) system is worth it in the light of some recent works¹¹ that showed the possibility of collisional excitation in an SB system. Indeed, under higher rare

gas partial pressure and low acoustic pressure, the usually featureless SBSL spectrum bears emission lines of excited species such as OH and Na; the presence of the Na line in SBSL spectra clearly indicates Na^+ reduction and Na atom excitation by collisions in SB, either inside the bubble or at its interface.^{11b}

In addition, the quest for the US frequency effect is made fascinating by the fact that excitation of Ln^{3+} does not always lead to light emission as quenching may also occur. Quenching by water molecules of the Ln^{3+} hydration shell is well known and occurs by coupling of the excited f-electron energy levels with OH vibrational overtones.¹² This quenching mode is reflected in the classical photoluminescence yield. Other types of quenching may also occur and are enhanced under ultrasound: excited species can be quenched by sonolytical products,¹³ excitation to the next nonemitting state is favored in the overheated zone around cavitation bubbles¹⁴ and so is collisional (Stern–Volmer) quenching.^{1a} This additional quenching explained the relatively low SL efficiency of UO_2^{2+} ions even in strongly complexing phosphoric acid medium¹³ and can also explain the observation made by Sharipov et al.^{9b} that Tb^{3+} SL increased by a factor of 4 in heavy water, whereas its classical PL increased by a factor of 10.

This article focuses on the studies of lanthanide ions excitation (Ce^{3+} , Tb^{3+} , Gd^{3+} , and Eu^{3+}) by US in a multibubble system at 20, 203, and 607 kHz and in a single-bubble system at 27 kHz under usual degassed conditions or under conditions

Received: December 7, 2012

Revised: February 18, 2013

Published: February 19, 2013



favoring line emission (i.e., collisions). Quantum yields (QYs) of SL are calculated whenever possible; the excitation mechanism is derived and the amount of quenching is estimated.

2. EXPERIMENTAL METHODS

The SBSL setup is a cylindrical quartz cell with a driving frequency of 27 kHz and a sample volume of 106 mL. Spectra are measured by an Acton Research SP-300i imaging spectrometer coupled to a charge-coupled-device detector (PIXIS 100B, Princeton Instrument). They are averaged for reproducibility and corrected for background noise and for the sensitivities of the gratings and CCD. The acoustic pressure was detected with a needle hydrophone ~ 2 mm above the position of the bubble. More experimental details of setups and procedures were recently reported.^{11b}

The MBSL setup consists of a thermostatted cylindrical reactor that is mounted on top of the high-frequency transducer operating at 203 or 607 kHz, (L3 communications ELAC Nautik). Ultrasonic irradiation with low-frequency ultrasound of 20 kHz was performed with a titanium horn (Vibra-Cell) placed reproducibly on top of the reactor. The acoustic power transmitted to the solution was measured with a thermal probe.^{10b} The sample volume of 250 mL was continuously sparged with Ar (Air Liquide, 99.999%) at a constant gas flow rate of 90 mL/min. The cryostat temperature was set to have a steady-state temperature of 10 to 11 °C within the sonoreactor during the ultrasonic treatment. Each spectrum is the average of at least three 300 s spectra corrected for background noise and for the quantum efficiencies of the gratings and CCD given by the manufacturer. Further details were previously reported.^{10c}

For all solutions, Milli-Q deionized water (0.055 $\mu\text{S}/\text{cm}$) was used. The solutions of hydrated Ln(III) were prepared by dissolving the hydrates of EuCl_3 , CeCl_3 , GdCl_3 , or TbCl_3 (all Alfa Aesar, REO 99.9%) in water. The pH was then adjusted to 1 to 2 with 1 M HCl (reagent grade) to avoid Ln(III) hydrolysis. The Ln(III)-chelate solutions were prepared by adding citric acid to the Ln(III) solution and then adjusting the pH to 8.4 to 9.3 with tetramethylammoniumhydroxide (TMAOH).

Light absorption and photoluminescence measurements were carried out using a 1 cm quartz cuvette. Absorption spectra were recorded with a Varian CARY 50 UV-vis spectrophotometer and fluorescence/phosphorescence spectra with a Fluoromax 4 from Jobin Yvon. The emission spectra were corrected for emission and excitation using the manufacturer sensitivity curves.

3. RESULTS AND DISCUSSION

3.1. Cerium(III). Solutions of CeCl_3 0.1 M were studied at 20 and at 203 kHz. The MBSL spectra at both frequencies are very similar and show Ce^{3+} total light absorption below 314 nm and an intense and large Ce^{3+} emission peaking at 349 nm on top of the SL continuum (Figure 1), in good agreement with spectra from the literature.^{6,9d} The SL QY was calculated as defined by Sharipov et al.^{9d} by subtracting a water spectrum from the Ce^{3+} SL spectrum and dividing the emission area by the absorption area. (See Figure 1SI in the Supporting Information.) Prior to this procedure, both spectra were extrapolated to 200 nm to take into account absorbed light in the wavelength interval nonaccessible to our measurements (below 235 nm). Obtained SL yields amount to 0.9 ± 0.1 at

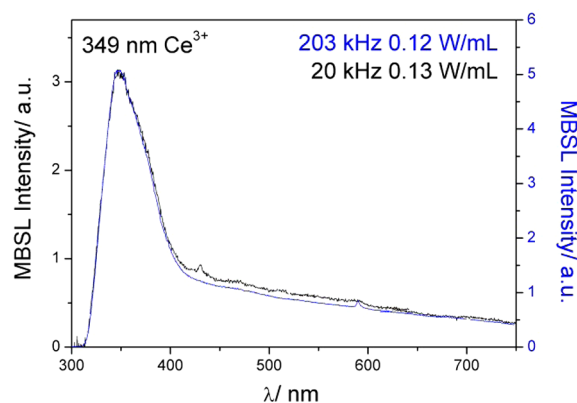


Figure 1. MBSL spectra of a 0.1 M CeCl_3 solution obtained at 20 and 203 kHz.

203 kHz whatever the acoustic power in the range of 0.11 to 0.21 W/mL and to 0.4 ± 0.1 at 20 kHz. The 203 kHz value is in very good agreement with the photoexcitation yield of 1. Therefore, MBSL of Ce^{3+} appears to arise from sonophotoexcitation and can be attributed to SPL. Actually, the only previous study of Ce^{3+} SL, performed by Sharipov et al. at 20 kHz in air⁶ and under Ar^{9d} led to SL QYs of 0.84 and 0.83, respectively. However, these values were overestimated due to not taking into account the UV part of the SL spectra (< 300 nm) properly, thus neglecting approximately half of the absorbed photons. This correction leads to good agreement between the presently determined yield at 20 kHz and Sharipov's one.

As indicated by the nearly 1 QYs in both classical photoexcitation and in 203 kHz SL, excited Ce^{3+*} is not subject to nonradiative de-excitation by coupling with OH vibration of surrounding water molecules or H_2O_2 formed by sonolysis due to the large energy gap between the emitting state and the next lower lying state¹⁵ and to the short lifetime (0.04 μs) of the excited state.¹⁴ However, in the close area around the collapsing bubbles, enhanced Stern–Volmer quenching (by collisions with sonolytical products, with the relatively concentrated chloride ions or with argon) and oxidative quenching by H_2O_2 may also occur. This can explain the lower QY obtained at low ultrasonic frequency because 20 kHz bubbles present a 100 times larger interface compared with 203 kHz ones.

To confirm the sonophotoexcitation mechanism of Ce^{3+} , we measured the SBSL of a 0.5 M CeCl_3 solution under conditions favorable to collisional excitation, that is, after pre-equilibration with 70 mbar of Ar^{11} . An intense Ce^{3+} emission was observed in the whole acoustic pressure range of SBSL, moreover, increasing proportionally to the intensity of the SL continuum (Figure 2SI in the Supporting Information), indicating photon excitation rather than collisional excitation. The calculated SBSL QY is $\sim 0.7 \pm 0.1$ whatever the acoustic pressure, in good agreement with MBSL results and with the photoexcitation QY.

3.2. Gadolinium(III). Sharipov et al.^{9a} observed in their MBSL studies (20 kHz, air, 1 M GdCl_3) a very intense emission around 309 nm, which they attributed to SL of Gd^{3+} . However, we were unable to reproduce this observation. Apart from Gd^{3+} absorption lines, the MBSL spectrum was not different from water emission either with 20 kHz or with 203 or 609 kHz US. Thus, considering a photoluminescence yield of 0.18¹⁴ and a relatively efficient collisional excitation,^{9a} it appears that Gd^{3+} excited state is most probably efficiently quenched. The

probability of Gd^{3+*} quenching by H_2O or H_2O_2 is very low due to the very large energy gap between the emitting state and the next lower energy state of Gd^{3+} .¹⁵ Therefore, Marcantonatos et al.¹⁶ proposed another quenching mechanism based on the loss of two inner-sphere coordinated water molecules and subsequent conversion of the resulting species to a hydrolyzed species that would form an exciplex. A second nonradiative de-excitation mechanism has to be considered due to the long (2.3 ms)¹⁴ lifetime of Gd^{3+*} : thermally activated promotion to the close-lying higher electronic level above the phosphorescent one.¹⁵ It is to be noted that both of these processes (dehydration and thermal activation) would be favored at the overheated bubble interfaces.

To reduce the amount of nonradiative decay, citrate was added to the Gd^{3+} solution: among several complexing agents, citrate showed the highest enhancement of Ln^{3+} light emission intensity.¹⁷ Photoluminescence spectra showed a 100-fold emission increase after the addition of citrate. The corresponding SL spectrum bore clear Gd^{3+} emission (Figure 2) and

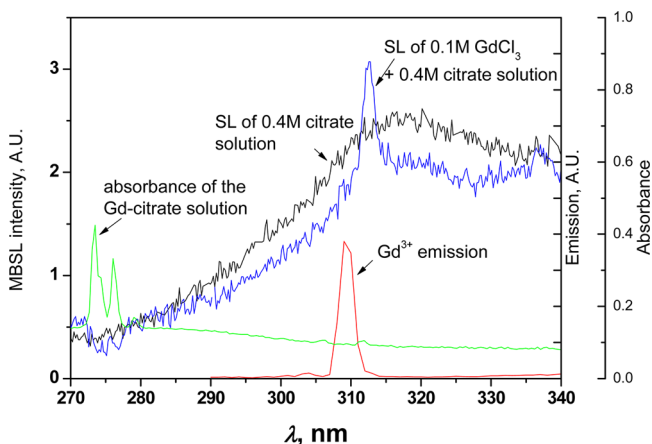


Figure 2. MBSL spectra of a solution of 0.4 M citrate alone (black) and of a solution of 0.1 M GdCl_3 + 0.4 M citrate (blue), 203 kHz, 0.12 W/mL. Absorption spectrum (green) of the Gd-citrate solution and fluorescence spectrum (red) of the GdCl_3 solution.

shifted to 310 nm by complexation. This confirms the excitation of Gd^{3+} under US (although the QY and consequently the excitation mechanism cannot be determined) and its significant quenching. The origin of the line reported by Sharipov et al.⁷ remains unknown.

3.3. Terbium(III). Figure 3 shows SBSL spectra of a degassed 0.1 M TbCl_3 solution at different acoustic pressures. Similar spectra were obtained when the solution was first equilibrated with 70 mbar Ar. The QY of SL was determined as previously for Ce^{3+} and is $\sim 2\%$ for both 1 mbar (standard SBSL conditions) and 70 mbar (gas conditions favorable to collisional excitation) Ar amounts, decreasing with increasing acoustic pressure (degassed solution: from 0.033 to 0.020 for Pac 1.12 to 1.30 bar; solution equilibrated with 70 mbar Ar: from 0.029 to 0.012 for Pac from 1.20 to 1.30 bar). This QY is lower than the photoluminescence yield of 0.08,¹⁴ and thus Tb^{3+} SBSL can be assigned to photoexcitation. Pure photoexcitation, even combined with quenching by water molecules, would lead to a constant ratio of 0.08 whatever the Ar content and the acoustic pressure. However, the QY of Tb^{3+} SBSL is lower at higher (70 mbar) Ar content, and for both gas contents it decreases when P_{ac} increases. This decrease is most probably due to higher

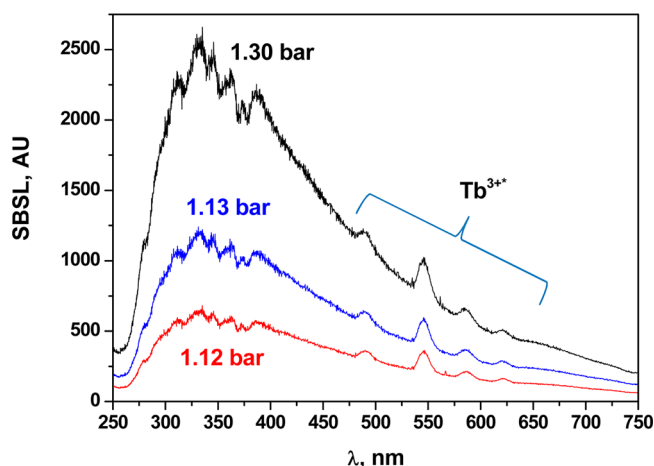


Figure 3. SBSL spectra of a degassed 0.1 M TbCl_3 solution at different acoustic pressures.

efficiency of nonradiative deactivation in the overheated zone around the bubble. The bubble is larger at higher P_{ac} and at higher Ar content,¹⁸ which correlates with the trend followed by the SBSL QY.

Figure 4 shows MBSL spectra of a 0.1 M TbCl_3 solution sparged with Ar at US frequencies of 20, 203, and 607 kHz. The

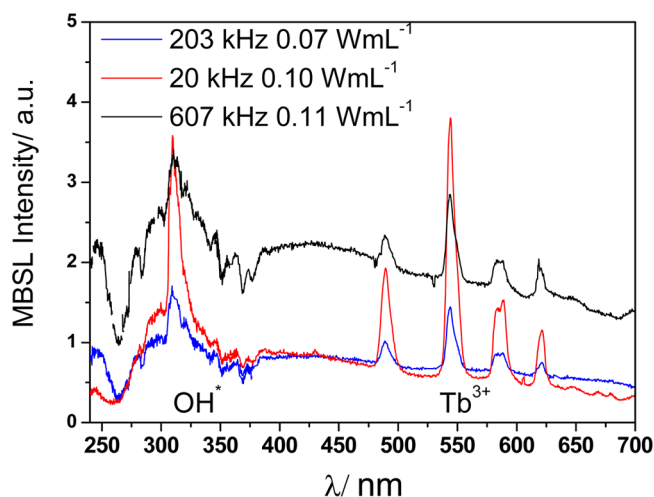


Figure 4. MBSL spectra of a 0.1 M TbCl_3 solution at 20, 203, and 607 kHz.

emission of Tb^{3+} is clearly visible at all three frequencies. Calculated QYs are of ~ 0.40 at 20 kHz, ~ 0.20 at 203 kHz, and ~ 0.10 at 607 kHz, in any case larger than the PL QY of 0.08, therefore indicating a large contribution of collisional excitation. Actually, these QYs, quantified as the ratio of emitted to absorbed areas, presume photoexcitation as the major mechanism while Tb(III) emission arises from two processes: photoexcitation and collisional excitation. Therefore, a better definition of QY in SL (hereafter named QY^{US}) should take into account both excitation mechanisms. Photoexcitation is proportional to the number of light emitting bubbles, N , to their volume proportional to r^3 and to the photon density; this can be summarized as photoexcitation being proportional to the SL intensity I_{SL} . Excitation by collisions is considered to occur at the bubble interface (and not in the bubble cores via droplet injection because Ln^{3+} would form nonluminescent

species at the high temperatures reached in the core at collapse); it is proportional to N , to the bubble/solution interface area (r^2), and to the density of hot particles formed in the bubbles; in other words it is proportional to the SL intensity, I_{SL} , divided by r . Thus, total excitation is proportional to $A_1 \times I_{SL} + A_2 \times I_{SL}/r$, where A_1 and A_2 are constants that quantify the relative efficiencies of excitation by photons and by collisions. The US quantum yield QY^{US} can then be defined for each US frequency as

$$\begin{aligned} QY^{US} &= \frac{\text{emission}}{\text{excitation}} \\ &= \frac{\text{emission}}{A_1 \times I_{SL} + A_2 \times I_{SL}/r} \\ &= \frac{\text{emission}}{A_1 \times I_{SL}(1 + B/r)} \\ &= \frac{QY^{obs}}{1 + B/r} \end{aligned} \quad (1)$$

where B/r is the part of the collisional excitation mechanism relative to photoexcitation ($B = A_2/A_1$) and QY^{obs} is the QY defined previously as in classical photoexcitation.

Written for all three frequencies with bubble radii normalized to the natural resonance radius of a bubble at 607 kHz with 4.6 μm ($B' = B/r_{607\text{kHz}}$), this gives:

$$QY_{20\text{kHz}}^{US} = \frac{0.40}{1 + B'/30} \quad (2)$$

$$QY_{203\text{kHz}}^{US} = \frac{0.20}{1 + B'/3} \quad (3)$$

$$QY_{607\text{kHz}}^{US} = \frac{0.10}{1 + B'} \quad (4)$$

For the bubble size, the natural resonance size¹⁹ was taken because the radius at collapse is not well known. This approximation is valid insofar as relative values are considered for radii and the aim of this work is to estimate the proportion of each excitation mechanism and of quenching for each US frequency and not to determine accurate values.

Each QY^{US} can also be expressed^{1a} as the ratio of the radiative deactivation rate constant k_{rad} to the sum of the rates of all deactivation processes, including radiative and non-radiative processes, namely, quenching by H_2O expressed by $k_{\text{H}_2\text{O}}$ and deactivation due to the presence of cavitation bubbles, k_{US} , comprising enhancement of nonradiative deactivation (by Stern–Volmer collisional quenching and/or by excitation to the next nonemitting state) at the overheated bubble interface and chemical quenching by sonolysis products, in particular, by sonolytical products issued from chloride anions,²⁰ whose concentration in the studied solutions is at least three times that of Tb^{3+} :



Both radicals (Cl^\bullet , $\text{HClO}^\bullet-$) are strong oxidants thus able to quench Tb(III) excited state via oxidation to Tb(IV) . The QY^{US} can thus be written as:

$$QY^{US} = \frac{k_{rad}}{k_{rad} + k_{\text{H}_2\text{O}} + k_{US}} \quad (7)$$

Normalization of all deactivation rate constants to k_{rad} yields:

$$QY^{US} = \frac{1}{1 + k_{\text{H}_2\text{O}}^r + k_{US}^r} \quad (8)$$

In the particular case of photoexcitation, this equation gives:

$$QY^{PL} = QY^{obs} = \frac{1}{1 + k_{\text{H}_2\text{O}}^r} \quad (9)$$

To determine the values of the eight unknowns (QY^{US} and k_{US}^r each at the three US frequencies, B' , and $k_{\text{H}_2\text{O}}^r$) one more equation is needed. To get it, we measured Tb^{3+*} emission after complexation by citrate at 20 and 203 kHz US. Because citrate absorbs in the UV, the QY^{obs} cannot be measured anymore. Alternatively, the ratio of the height of Tb^{3+*} main emission peak at 544 nm (h_{544}) to the continuum intensity at 450 nm (I_{450}) is taken as measure of the yield of emission, where I_{450} serves as measure of the cavitation intensity. This ratio has the advantage of being independent from the number of active bubbles; I_{450} is proportional to the bubble volume, that is, r^3 , h_{544} to the bubble surface, thus r^2 , because the main excitation mechanism is by collisions. Therefore, the ratio is proportional to $1/r$. Obtained values for the aqua and the citrate complexes are summarized in Table 1.

Table 1. Ratio of Tb^{3+*} Main Peak Height h_{544} to the Continuum Intensity I_{450} for 20, 203, and 607 kHz; Solutions of TbCl_3 and Terbium Citrate Complex

US frequency	h_{544}/I_{450}	
	TbCl_3 solution	Tb citrate solution
20 kHz	4.0 ± 0.3	12.2 ± 0.3
203 kHz	0.86 ± 0.17	1.4 ± 0.2
607 kHz	0.48 ± 0.02	

Complexation increases Tb^{3+} relative emission by a factor of 3 at 20 kHz and 1.5 at 203 kHz. The comparison of the emission yields of the aqua and citrate complexes at 20 and 203 kHz gives, assuming that citrate prevents quenching by water molecules but does not modify too much the collisional excitation efficiency:

$$\frac{12.2}{4.0} QY_{20\text{kHz}}^{US} = \frac{1}{1 + k_{US20\text{kHz}}^r} \quad (10)$$

$$\frac{1.4}{0.86} QY_{203\text{kHz}}^{US} = \frac{1}{1 + k_{US203\text{kHz}}^r} \quad (11)$$

The first equation is used to complete the equation system, and the second equation is used to check the obtained results. Numerical resolution of the system of eight equations and eight unknowns yields the values given in Table 2. Solving eq 11 using the so-determined value of $k_{US203\text{kHz}}^r$ yields a value of $QY_{203\text{kHz}}^{US} = 0.22\%$ in satisfactory agreement with the previously computed value of 0.34%. The obtained value of B' confirms the predominant part of the collisional excitation mechanism: $B/r = 5.8$ at 20 kHz, 58 at 203 kHz and 175 at 607 kHz.

Calculated US QYs (less than 1% at high frequency) are smaller than the photoexcitation one of 8%: $QY^{PL} > QY_{20\text{kHz}}^{US} > QY_{203\text{kHz}}^{US} > QY_{607\text{kHz}}^{US}$. This is due to intense quenching as indicated by the high values of k_{US}^r , especially at high frequency. As already mentioned, this quenching decomposes into chemical quenching (oxidation to Tb(IV)) by sonolytical

Table 2. Calculated Values of Tb³⁺ MBSL Quantum Yields and of the Corresponding Nonradiative Deactivation Rate Constants^a

QY _{20kHz} ^{US}	QY _{203kHz} ^{US}	QY _{607kHz} ^{US}	B'	k _{H₂O} ^r	k _{US20kHz} ^r	k _{US203kHz} ^r	k _{US607kHz} ^r
(5.84 ± 0.77) 10 ⁻²	(3.36 ± 0.52) 10 ⁻³	(5.67 ± 0.89) 10 ⁻⁴	175 ± 31	11.5	4.61 ± 2.37	285 ± 53	1750 ± 314

^aGiven uncertainties are the standard deviations obtained after 1000 numerical calculations of the system of eight equations, whereby the variables were allowed to vary randomly in an interval defined by their value and uncertainty.

products and heat-enhanced Stern–Volmer collisional quenching or excitation to the next nonemitting state, but unfortunately it is hard to determine experimentally the ratio of each pathway. The larger surface-to-volume ratio at higher frequency favors all three of them.

It is to be noted that Tb³⁺ is much more sensitive to quenching than Ce³⁺, which can be traced back to the smaller energy gap between Tb³⁺ emitting state and its next lower state and to the very short lifetime of Ce^{3+*} (~0.04 μs, to be compared with ~430 μs for Tb³⁺). Eu^{3+*} has a smaller energy gap and is known to be very sensitive to quenching by O–H vibrations;¹⁵ besides, it is expected to also be sensitive to strong US-induced quenching, like Tb³⁺, due to its long lifetime (~110 μs).

3.4. Europium(III). In agreement with these expectations, SBSL spectra of 0.1 M EuCl₃ solutions showed no Eu³⁺ emission. In the presence of citrate, tiny peaks could be observed, identical to those obtained under photoexcitation. Besides, in their 20 kHz MBSL experiments, Sharipov et al.^{9c} could not observe Eu³⁺ emission in light water so that they turned to heavy water, where nonradiative deexcitation is far less. (OD is a poor quencher when compared with OH.) Moreover, Eu^{3+*} can also be quenched by sonolytically produced H₂O₂. Indeed, lanthanides and uranyl ions have very similar chemistries, and, in particular, the redox potentials of UO₂²⁺/UO₂⁺ and Eu³⁺/Eu²⁺ are close (0.062, respectively, –0.36 V for the ions in their fundamental state). In a recent study of uranyl SL,¹³ Pflieger et al. showed that the excited uranyl ion UO₂^{2+*} can be efficiently quenched by H₂O₂ through the reaction UO₂^{2+*} + H₂O₂ → UO₂⁺ + H⁺ + HO₂[•], where uranium is reduced from +VI to +V.

In the present study, Eu³⁺ was protected from quenching by complexation with citrate. Indeed, complexed Eu³⁺ shows sonoluminescence, and the obtained spectrum (Figure 3SI in Supporting Information) corresponds to the classical photoexcitation one. The ratios of the main emission peak heights (at 592 and 699 nm) to the continuum intensity taken at 500 nm show no influence of the acoustic power or of the US frequency (203 or 607 kHz).

4. CONCLUSIONS

The sonoluminescence of Ce³⁺, Tb³⁺, Gd³⁺, and Eu³⁺ was measured in single-bubble and multibubble (at US frequencies of 20, 203, and 607 kHz) systems. All of these ions can be excited by US, but quenching decreases their emission to an extent much larger than in classical photoluminescence: indeed, the efficiency of nonradiative de-excitation pathways (Stern–Volmer collisional quenching, excitation to the next nonemitting state) is increased in the overheated zone of the collapsing bubbles, and new quenching pathways like chemical quenching by sonolysis products (e.g., Cl[•], HClO[•], H₂O₂) may have to be considered when the luminescent ions are exposed to ultrasound.

The main excitation mechanism was shown to be photoexcitation for Ce³⁺ in both SBSL and MBSL, collisional

excitation for Tb³⁺ in MBSL, and photoexcitation for Tb³⁺ in SBSL. The latter example shows that even under favorable conditions collisional excitation plays a much less important role in SBSL than in MBSL. Identification of the excitation mechanism of Gd³⁺ and Eu³⁺ was not possible due to very faint (if any) emission in aqueous chloride solutions. Complexation of Ln³⁺ by citrate increases the SL yields by protecting the excited ions from quenching by OH vibrations and by products of sonolysis: after complexation, all ions exhibit emission spectra similar to the classical photoluminescence ones. In a detailed study of Tb³⁺ MBSL, QYs suited to the emission under US were defined to take into account both excitation mechanisms and all types of quenching. The collisional excitation mechanism was shown to prevail, and its contribution was shown to increase greatly with the US frequency.

■ ASSOCIATED CONTENT

Supporting Information

Comments on the specificity of the SL QY, its determination for Ce³⁺ (0.1M) at 203 kHz, evolution of Ce³⁺ emission with increasing continuum emission in SBSL, and MBSL spectra of a 0.1 M solution of Eu³⁺ citrate. This material is available free of charge via the Internet at <http://pubs.acs.org>.

■ AUTHOR INFORMATION

Corresponding Author

*Institut de Chimie Séparative de Marcoule (ICSM), UMR 5257 CEA/CNRS/UM2/ENCSCM, BP 17171, 30207 Bagnols-sur-Cèze, France. Tel: +33 (0) 4 66 33 92 50. Fax: +33 (0) 4 66 79 76 11. E-mail: rachel.pflieger@cea.fr.

Present Address

§Julia Schneider: III Physikalisches Institut, Friedrich-Hund-Platz 1, 37077 Göttingen, Germany.

Author Contributions

||Rachel Pflieger and Julia Schneider contributed equally.

Notes

The authors declare no competing financial interest.

■ ACKNOWLEDGMENTS

This work was performed in the framework of the European Associated Laboratory LEA SONO between CNRS and MPG.

■ ABBREVIATIONS

SL, sonoluminescence; SBSL, single-bubble sonoluminescence; MBSL, multibubble sonoluminescence; SPL, sonophotoluminescence; QY, quantum yield; US, ultrasound

■ REFERENCES

- (1) (a) Bünzli, J. C. G. *Chem. Rev.* **2010**, *110*, 2729–2755. (b) Kagan, H. B. *Inorg. Chim. Acta* **1987**, *140*, 3–6.
- (2) (a) Godfrey, E. M.; Rushbrook, S. M.; Carrol, N. R. *Postgrad. Med. J.* **2010**, *86*, 346–353. (b) ter Haar, G. *Prog. Biophys. Mol. Biol.* **2007**, *93*, 111–129.

- (3) (a) Baig, R. B. N.; Varma, R. S. *Chem. Soc. Rev.* **2012**, *41*, 1559–1584. (b) Bang, J. H.; Suslick, K. S. *Adv. Mater.* **2010**, *22*, 1039–1059.
- (4) Suslick, K. S.; Skrabalak, S. E. Sonocatalysis. In *Handbook of Heterogeneous Catalysis*; Ertl, G., Knözinger, H., Schüth, F., Weitkamp, J., Eds.; Wiley-VCH: Weinheim, 2008; Vol. 4.
- (5) Ashokkumar, M.; Grieser, F. *Chem. Commun.* **1998**, *5*, 561–562.
- (6) Sharipov, G. L.; Gainetdinov, R. K.; Abdrakhmanov, A. M. *Russ. Chem. Bull.* **2003**, *52*, 1969–1973.
- (7) Sharipov, G. L. *JETP Lett.* **2007**, *85*, 458–460.
- (8) Sharipov, G. L.; Kazakov, V. P. *Opt. Spektrosk.* **1980**, *48*, 69–74.
- (9) (a) Sharipov, G. L.; Gainetdinov, R. K.; Abdrakhmanov, A. M. *Russ. Chem. Bull.* **2005**, *54*, 1383–1386. (b) Sharipov, G. L.; Gainetdinov, R. K.; Abdrakhmanov, A. M. *Russ. Chem. Bull.* **2006**, *55*, 1114–1118. (c) Sharipov, G. L.; Gainetdinov, R. K.; Abdrakhmanov, A. M. *Russ. Chem. Bull.* **2008**, *57*, 1827–1830. (d) Sharipov, G. L.; Gainetdinov, R. K.; Abdrakhmanov, A. M. *Russ. Chem. Bull.* **2008**, *57*, 1831–1836. (e) Sharipov, G. L.; Gareev, B. M.; Abdrakhmanov, A. M. *JETP Lett.* **2010**, *91*, 566–569.
- (10) (a) Beckett, M. A.; Hua, I. J. *Phys. Chem. A* **2001**, *105*, 3796–3802. (b) Navarro, N. M.; Chave, T.; Pochon, P.; Bisel, I.; Nikitenko, S. I. *J. Phys. Chem. B* **2011**, *115*, 2024–2029. (c) Ndiaye, A. A.; Pflieger, R.; Siboulet, B.; Molina, J.; Dufreche, J. F.; Nikitenko, S. I. *J. Phys. Chem. A* **2012**, *116*, 4860–4867.
- (11) (a) Liang, Y.; Chen, W. Z.; Xu, X. H.; Xu, J. F. *Chin. Sci. Bull.* **2007**, *52*, 3313–3318. (b) Schneider, J.; Pflieger, R.; Nikitenko, S. I.; Shchukin, D.; Mohwald, H. *J. Phys. Chem. A* **2011**, *115*, 136–140. (c) Young, J. B.; Nelson, J. A.; Kang, W. *Phys. Rev. Lett.* **2001**, *86*, 2673–2676.
- (12) (a) Horrocks, W. D.; Sudnick, D. R. *J. Am. Chem. Soc.* **1979**, *101*, 334–340. (b) Kropp, J. L.; Windsor, M. W. *J. Phys. Chem.* **1967**, *71*, 477–482.
- (13) Pflieger, R.; Cousin, V.; Barre, N.; Moisy, P.; Nikitenko, S. I. *Chem.—Eur. J.* **2012**, *18*, 410–414.
- (14) Beitz, J. V. Similarities and Differences in Trivalent Lanthanide- and Actinide-Ion Solution Absorption Spectra and Luminescence Studies. In *Handbook on the Physics and Chemistry of Rare Earths: Lanthanides/Actinides: Chemistry*; Gschneidner, K. A., Eyring, L., Jr., Choppin, G. R., Lander, G. H., Eds.; Elsevier Science: New York, 1994; Vol. 18, pp 159–195.
- (15) Stein, G.; Wurzburg, E. *J. Chem. Phys.* **1975**, *62*, 208–213.
- (16) Marcantonatos, M. D.; Deschaux, M.; Vuilleumier, J. J.; Combremont, J. J.; Weber, J. J. *Chem. Soc., Faraday Trans. 2* **1986**, *82*, 609–629.
- (17) Poluektov, N. S.; V., Z. Y.; Zhikareva, E. A.; Mishchenko, V. T. *Zh. Prikl. Spektrosk.* **1972**, *17*, 67–70.
- (18) Hopkins, S. D.; Putterman, S. J.; Kappus, B. A.; Suslick, K. S.; Camara, C. G. *Phys. Rev. Lett.* **2005**, *95*, 25.
- (19) Mason, T. J.; Lorimer, J. P. *Applied Sonochemistry. The Uses of Power Ultrasound in Chemistry and Processing*; Wiley-VCH: Weinheim, Germany, 2002.
- (20) Harada, H. *Int. J. Hydrogen Energy* **2001**, *26*, 303–307.